

## Supporting Information

### Orthogonal protein decoration of DNA nanostructures based on SpyCatcher-SpyTag interaction

*Sandra Kröll, Leonie Schneider, Parvesh Wadhvani, Kersten S. Rabe, and Christof M. Niemeyer\**

#### Experimental Section

##### Synthesis and characterization of SpyTag003 peptide

All reagents for the peptide synthesis such as the solid phase, Fmoc-protected amino acids, coupling reagents, base and solvents were purchased either from Merck Biosciences or Iris Biotech and used without further purification. 2-(2-azidoethoxy)ethoxy]acetic acid was purchased as cyclohexylamine salt from Iris Biotech. The peptide was synthesized on an automated Syro II multiple peptide synthesizer (MultiSynTech), on a Rink amide MBHA resin on a 100  $\mu\text{mol}$  scale using standard Fmoc solid phase peptide synthesis protocols. Each amino acid was double coupled using 4 eq. excess of the Fmoc protected amino acids (400  $\mu\text{mol}$ ) in presence of 4 eq. of 2-(1H-benzotriazole-1-yl)-1,1,3,3-tetramethyluronium hexafluorophosphate (HBTU, 400  $\mu\text{mol}$ ), and 4 eq. of 1H-1,2,3-Benzotriazol-1-ol (HOBt, 400  $\mu\text{mol}$ ), and 8 eq. of N-Ethyl-N-(propan-2-yl)propan-2-amine (DIPEA, 800  $\mu\text{mol}$ ). Coupling of 2-(2-azidoethoxy)ethoxy]acetic acid to the N-terminus was performed using 5 eq. 2-(2-azidoethoxy)ethoxy]acetic acid (500  $\mu\text{mol}$ ) in the presence of dicyclohexylcarbodiimide (DIC, 500  $\mu\text{mol}$ ) and HOBt (50  $\mu\text{mol}$ ) over 18 h coupling time in dimethylformamide as solvent. Crude peptides were obtained by cleaving the peptides from the solid support by using a solution of cleavage cocktail containing TFA:H<sub>2</sub>O:triisopropylsilane:phenol:thioanisole:ethanedithiol in the ratio of 77.5:5:5:5:5:2.5 (v/v) for 2 h. The solid support was filtered off and the resulting solution was gently evaporated under nitrogen stream. The resulting viscous solution was taken in ice-cold Et<sub>2</sub>O and centrifuged at 8000 rpm at 4 °C for 5 min. Analytical chromatogram of the crude peptide revealed the presence to two peaks at 12.3 and 12.8 min with a mass difference of about 16 amu between the expected (12.8 min) product and the oxidized product. The crude peptides were purified using a high-pressure liquid chromatography (HPLC) system from JASCO on a semi-preparative Vydac C18 column equilibrated at 35°C, using a water/acetonitrile gradient supplemented with 0.1 % (v/v) trifluoroacetic acid such that the desired product was separated from the oxidized product. The purified peptides were characterized using an analytical LC (Agilent) coupled to an ESI mass spectrometer (QTOF, Bruker) and were found to be over 95% pure.

##### Synthesis and purification of SpyTag003-oligonucleotide

The oligonucleotides equipped with 5'-SCO and 3'-Cy3 were purchased from Biomers and used without further purification. A slight excess of 4.6 nmol of oligonucleotide was incubated with 4 nmol of azide-modified ST peptide for 6 h at 55°C in H<sub>2</sub>O as previously reported to facilitate the SPAAC reaction.<sup>1</sup> Reversed phase HPLC was conducted for purification of the generated ST-modified oligonucleotides using a bioinert Agilent technologies 1260 infinity II system equipped with a Poroshell 120 EC-C18 2.7  $\mu\text{m}$  column (4.6 x 150 mm, Agilent). A linear gradient of 5-50% acetonitrile in 0.1 M triethylammonium acetate over 30 min at a flow rate of 0.5 mL/min was used and products were detected at 260 nm and

280 nm. The concentration of the resulting ST-oligonucleotide conjugates was determined by UV-Vis spectroscopy using the molar extinction coefficient of the incorporated Cy3 label at 550 nm ( $150\,000\text{ M}^{-1}\text{ cm}^{-1}$ ). The calculated yield of the reaction was between 25% and 40%.

### **Characterization of ST-modified staples**

The HPLC-purified ST-modified oligonucleotides were mixed with 4x SDS loading dye (500 mM Tris, 20% v/v Glycerin, 4% SDS v/v, 5%  $\beta$ -Mercaptoethanol v/v, 0.5% Bromophenol blue w/v, pH 6.8) and analyzed by a 4-15% SDS-PAGE gradient gel (Mini-Protean TGX Gels (4-15%), BioRad) in Maniatis buffer (25 mM Tris-base, 25 mM Glycine, 5% SDS v/v). Gels were run at 120 V and bands were subsequently visualized by fluorescence imaging of the incorporated Cy3 labels.

### **Design of rectangular DNA origami nanostructures**

The DNA origami nanostructures (DON) were synthesized using the single stranded scaffold p7560 (Tilbit nanosystems) and 240 staple oligonucleotides as previously described.<sup>2</sup> Several staples were modified to incorporate five Cy5 groups for electrophoresis, three ligands with 5'-ST for coupling of SC-fusion proteins and 3'-Cy3 for electrophoresis, as well as three Biotin-modified linkers for bead-assisted purification. All unmodified, Cy5-modified staples and Biotin-modified linkers were purchased from Sigma-Aldrich. The sequences are listed in Table S1.

### **Assembly and purification of DNA nanostructures**

DON were synthesized as previously reported<sup>3</sup> using 20 nM single stranded scaffold p7560 with a 10-fold molar excess of staple strand oligonucleotides in TEMg<sub>15</sub> buffer (20 mM Tris base, 1 mM EDTA, 15 mM MgCl<sub>2</sub>, pH 8.0). DON were annealed in a Thermocycler (Eppendorf Master cycler<sup>®</sup> pro), with a denaturation at 95 °C for 5 min and step-wise temperature decrease from 75 °C to 25 °C (cooling rate of - 0.1 °C/s). Excess staple strands were removed and DON were purified using PEG-precipitation according to Dietz's procedure<sup>4</sup> by mixing with an equal volume of precipitation buffer (5 mM Tris base, 1 mM EDTA, 505 mM NaCl, 15% PEG-8000) and centrifugation at 16.100 g for 30 min at 20°C. The resulting pellet was resuspended in 50  $\mu$ L TEMg<sub>6</sub> buffer (20 mM Tris base, 1 mM EDTA, 6 mM MgCl<sub>2</sub>, pH 8.0) for storage.

### **Quantification of DON via qPCR**

Quantitative PCR (qPCR) was used to determine concentrations of synthesized DON. A calibration curve was generated from serial dilutions of p7560 strand in the range of 15 nM - 150 fM in triplicates. 1.5  $\mu$ L p7560 calibration standards or DON samples were added to 20  $\mu$ L PCR-Mix. In 10 mL PCR-Mix, 1 mL 10x PCR buffer (160 mM ammonium sulfate, 670 mM Tris-HCl, 0.1% Tween 20, pH 8.8), 500  $\mu$ L KCl (50 mM), 600  $\mu$ L MgCl<sub>2</sub> (50 mM), 200  $\mu$ L dNTPs (10 mM each), 100  $\mu$ L primer FW\_p7560 (100  $\mu$ M, CCAACGTGACCTATCCATTAC), 100  $\mu$ L primer RV\_p7560 (100  $\mu$ M, TTCCTGTAGCCAGCTTTCATC), 20  $\mu$ L TaqMan3\_p7560 probe (100  $\mu$ M, FAM-CGACGGGTTGTTACTCGCTCACAT-TAMRA) and 100  $\mu$ L Taq DNA Polymerase (5 U/ $\mu$ L) (New England Biolabs) were combined in autoclaved H<sub>2</sub>O. Measurements were performed using a real-time thermocycler (Corbett research).  $\Delta$ Ct values were calculated by subtraction of the Ct signal (manually adjusted) from the maximal number of cycles ( $C_{Max}$ ). The  $\Delta$ Ct values were plotted against the log concentration of the p7560 calibration to yield the final DON concentrations by linear regression.

### Construction of plasmids

The plasmids were constructed by isothermal recombination according to Gibson,<sup>5</sup> using oligonucleotide primers with 30 bp homologous overlaps. pET22b-Gre2p was designed with C-terminal fusion and pET22b-ADH with a N-terminal fusion of the SC003-tag for bioconjugation as well as a Hexahistidin (His<sub>6</sub>)-tag for affinity purification. After assembly for 1 h at 50°C and digestion by DpnI, constructs were transformed into *E. coli* DH5α cells and selected on LB plates containing 100 µg/mL ampicillin at 37°C overnight (LB<sub>Amp</sub>). The plasmids were extracted from a liquid culture and purified using the ZR Plasmid Miniprep Classic Kit (Zymo Research) according to the manufacturer's instructions. Sequences were subsequently verified by commercial sequencing (LGC genomics). For primer sequences, see Appendix Table S4; for protein sequences, see Appendix Table S5.

### Protein expression and purification

For heterologous expression of the proteins, *E. coli* BL21(DE) cells were transformed with plasmids encoding for the respective tag-functionalized fusion protein and selected on LB<sub>Amp</sub>-plates at 37°C overnight. Liquid cultures from individual clones were prepared in 50 mL LB<sub>Amp</sub> and incubated for 16 h at 37°C and 180 rpm. 2 L LB<sub>Amp</sub> were inoculated with 40 mL culture and incubated at 37°C and 180 rpm until an OD<sub>600</sub> of 0.6 - 0.9. Subsequently, IPTG was added in a final concentration of 0.1 mM to induce protein expression at 25°C and 180 rpm overnight. The cells were harvested by centrifugation (10.000 g for 10 min), resuspended in NPI10 buffer (50 mM NaH<sub>2</sub>PO<sub>4</sub>, 300 mM NaCl, 10 mM Imidazole, pH 8.0) and frozen at -80°C. Thawed cells were treated with DNase and lysozyme for 30 min at room temperature. After disruption by ultrasonication, the lysed cells were centrifuged for 1 h at 45.000 g at 4°C and filtrated through a 0.45 µm Durapore PVDF membrane (Steriflip, Millipore) to yield the clear lysate. The pure proteins were obtained by Ni-NTA affinity chromatography on a FPLC Äkta Pure liquid chromatography system (GE Healthcare) with a HisTrap FF Ni-NTA column (GE Healthcare). Proteins were eluted with a linear gradient from 100% NPI10 buffer to 100% NPI500 buffer (50 mM NaH<sub>2</sub>PO<sub>4</sub>, 300 mM NaCl, 500 mM Imidazole, pH 8.0). The buffer was exchanged to PBS buffer using a 30 kDa cut-off centrifugal concentrator (Vivaspin, GE Healthcare). Proteins were analyzed by standard 12% SDS-PAGE and Coomassie staining and concentrations were determined by UV-Vis spectroscopy. The theoretical molar extinction coefficients at 280 nm were calculated by using the Geneious software (version 9.1.3).

### Kinetic analysis of conjugate formation via SDS-PAGE

DNA-protein conjugate formation of fusion enzymes with the ST-oligonucleotide was analyzed using SDS-PAGE by mixing 0.5 µM of Gre2p-SC or SC-LbADH, respectively, with 0.65 µM ST-modified oligonucleotide in T-TEMg<sub>12.5</sub> buffer (20 mM Tris base, 1 mM EDTA, 12.5 mM MgCl<sub>2</sub>, 0.01% v/v Tween 20, pH 7.6), according to the standard procedure implemented in our previous study of the Halo-Tag.<sup>6</sup> The reaction was stopped after 0, 2.5, 5, 10, 30, 60, 90 and 120 min incubation time at 30°C. Samples were incubated with 4 x SDS loading dye at 95°C for 5 min and analyzed by a 4-15% SDS-PAGE gradient gel in Maniatis buffer with PageRuler™ Prestained Protein Ladder (Thermo Fisher) as a mass reference. The DNA-protein conjugate formation was estimated by grey-scale analysis performed with Image J software and calculated as:

$$\text{Conjugate [\%]} = \frac{\text{peak area (conjugate)} * 100\%}{\text{peak area (conjugate)} + \text{peak area (unbound protein)}}$$

### **Immobilization of fusion proteins on DON**

Two or three molar equivalents of Gre2p-SC or SC-LbADH, respectively, per binding site (corresponding to 6 or 9 pmol) were incubated with 1 pmol DON in T-TEMg<sub>12.5</sub> at 30°C for up to 2 h. Samples were subsequently analyzed by agarose gel shift assay and AFM, as described below. DON with  $n = 0, 1, 2$  or 3 immobilized proteins were counted to assess the occupancy densities. Each sample was imaged at least twice, and a minimum of 100 DON were counted per sample. The distribution was plotted in bar diagrams and the average occupancy density was calculated as:

$$\text{Average Occupancy [\%]} = \frac{n(\text{proteins immobilized}) * 100\%}{n(\text{DON}) * \text{binding sites}}$$

### **AFM Measurements**

Depending on the concentration, the protein decorated DON were diluted up to 20-fold in TEMg<sub>12.5</sub> buffer (20 mM Tris base, 1 mM EDTA, 12.5 mM MgCl<sub>2</sub>, pH 7.6). 10  $\mu$ L of diluted sample were deposited onto a freshly cleaved mica platelet (Plano GmbH) for 3 min at room temperature. DON were imaged with SNL-10 cantilevers (0.35 Nm<sup>-1</sup>, Bruker) in liquid Tapping Mode on a MultiMode<sup>TM</sup> 8 atomic force microscope (Bruker) equipped with a NanoScope V controller. The scans were analyzed with NanoScope Analysis software (Bruker).

### **Electrophoretic analysis of DON**

Orange G 6x loading buffer (20% v/v Glycerin, 1% Orange G w/v in H<sub>2</sub>O) was added to the DON samples for 1% agarose gel electrophoresis. Agarose gels were run at 70 V at 4°C for 4 h in 0.5x TAEMg buffer (20 mM Tris base, 10 mM acetic acid, 1 mM EDTA, 6.25 mM Mg(AcO)<sub>2</sub>, pH 8.0) with Quick Load<sup>®</sup> 1 kb extended DNA Ladder (New England Biolabs) as a mass reference. Bands were visualized by fluorescence imaging of the incorporated Cy5 labels and subsequent staining with ethidium bromide.

### **Bead-assisted purification of protein-decorated DON**

In several cases, bead-assisted purification was conducted prior to AFM or activity analysis as previously described.<sup>7</sup> A typical experiment contained 100  $\mu$ g STV-coated microbeads (MBs) (Dynabeads<sup>TM</sup> M-280 Streptavidin, Invitrogen) and 1 pmol DON, equipped with Biotin-linker staples with an internal, cleavable disulfide bond. Up to 100 molar equivalents per binding site of the respective fusion enzyme was added in T-TEMg<sub>12.5</sub> reaction buffer and allowed to bind for up to 2 h at 30°C. After three washing steps, DON were released from the MBs by reductive cleavage of the biotin linker using 100 mM DTT for 20 min at 30°C.

### **Analysis of enzymatic activity immobilized with DNA-conjugate and DON**

Enzymatic activities of Gre2p and LbADH were determined using chiral HPLC analysis. The concentrations were determined prior to each experiment using the theoretical molar extinction coefficients at 280 nm as calculated by the Geneious software (version 9.1.3). For each enzyme, four samples were prepared: one containing the freely diffused enzyme (30 nM), one with the enzyme bound to the ST-oligonucleotide (30 nM), one with on-bead coupled and washed DON immobilized enzyme, as well as enzyme incubated with DON without binding sites (serving as negative controls). The reaction was started by addition of 5 mM NDK and 1 mM NADPH in a total volume of 100  $\mu$ L T-TEMg<sub>12.5</sub> and incubated for 5 h at 30°C. The reaction was stopped by extraction with 150  $\mu$ L ethyl acetate, of which 80  $\mu$ L were dried and analyzed with an HPLC (Agilent 1260 series) equipped with a

Diode Array Detector and chiral Lux 3 $\mu$ m Cellulose-1 column (Phenomenex) as previously described.<sup>8</sup> A 9:1 n-heptane/2-propanol mobile phase at a flowrate of 0.5 mL/min and at 10°C was used. The conversion of NDK was calculated using the signal intensities of NDK and the specific hydroxy ketones at 210 nm.

#### **Measurement of pH profiles of enzymes**

Activity assays were performed with enzymes in a final concentration of 50 nM, 5 mM NDK and 1 mM NADPH in 100 mM buffers with different pH values (Tris-HCl, pH 5.0 to 6.0; Tris base, pH 7.0 to 9.0; Carbonate-bicarbonate, pH 9.0 to 10.0) with 1 mM EDTA, 12.5 mM MgCl<sub>2</sub> and 0.01% v/v Tween 20 on a Synergy Plate reader (Nunc™ Microtiter plates Immuno PolySorp 96-Well, 30°C). Activities were determined by the conversion of NADPH, as indicated by the decrease of absorption at 340 nm. Blanks containing NADPH in the respective buffer were recorded and subtracted from the enzyme containing samples to account for degradation of NADPH.

#### **Enzyme detection *via* Western Blot**

After each activity experiment, enzyme amounts in the samples were determined to ensure that samples contained comparable amounts of enzymes as well as to verify successful conjugation to ST-DNA or DON, respectively. For this purpose, 4-15% SDS-PAGE was performed as described above and proteins were blotted onto a PVDF membrane in blotting buffer (25 mM Tris-Base, 192 mM Glycine, pH 8.3) at 300 mA and 4°C overnight. After blocking the membrane in 5% (w/v) milk powder in T-TBS (20 mM Tris-Base, 137 mM Sodium chloride, 0.1% Tween 20, pH 7.6) for 1 h at RT, the primary antibody (rabbit anti-SpyCatcher, BioRad; 1:10000 in 5% milk powder) was applied for 1 h at RT. The membrane was washed three times and incubated with the alkaline phosphatase-conjugated (AP) secondary antibody (goat-anti-rabbit-AP, Sigma-Aldrich; 1:5000 in 5% milk powder) for 2 h at RT. After three final washing steps, the protein bands were developed using Alkaline Phosphatase Conjugate Substrate Kit (BioRad) according to the manufacturer's instructions.

## Supplementary Figures

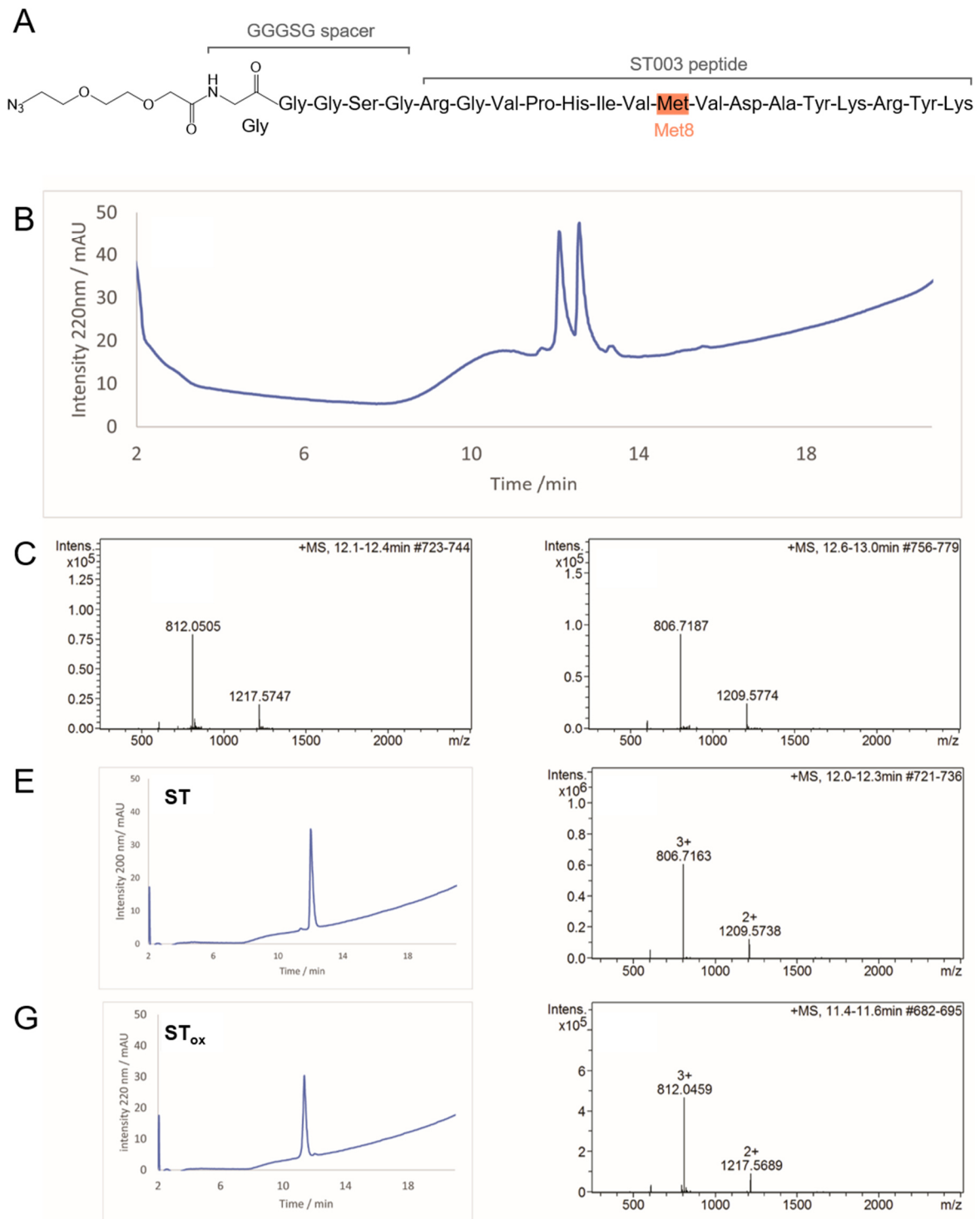


**Fig. S1** Characterization and purification of the synthesized ST003 peptide. **A)** Structure of the ST003 peptide equipped with N-terminal azide moiety and adjacent GGGSG linker. The ST peptide was changed in four amino acids and additionally appended by three amino acids from version 001 to version 003, resulting in the 16 amino acid ST003 peptide Arg-Gly-Val-Pro-His-Ile-Val-Met-Val-Asp-Ala-Tyr-Lys-Arg-Tyr-Lys. The linker was additionally introduced to increase the distance between the DON surface and the ST peptide to avoid steric and electrostatic hindrances between the negatively charged

DON and the SC domain, although it can be assumed that the ligation of the ST peptide on the DON surface with SC-fusion proteins is dominated by the ~400-fold faster reaction rate of the 003 variant. Indeed, in the key study,<sup>9</sup> Howarth and co-workers showed that the reaction between SC003 and ST003 proceeds with nearly diffusion-limited kinetics, exhibiting a second-order order constant which is about 400 times faster than that of the original SC/ST001 version. Interestingly, characterization of the SC/ST003 variant at different concentrations showed that the most significant difference from the SC/ST001 version occurs at low nanomolar concentrations. Since this is the concentration range used for protein coupling to DON, it stands to reason that the SC/ST001 system is generally not well suited for protein functionalization of DON. **B-H**) LC-MS chromatograms showing absorbance at 220 nm (**B, E, G**) and corresponding mass spectra (**C, D, F, H**) of crude and purified peptides. Appearance of two peaks in the crude chromatogram (**B**) between 12-13 min with a mass difference of 16 amu indicates oxidation of an amino acid in the peptide, most likely at methionine residue Met8, as previously reported for Fmoc peptide syntheses.<sup>10</sup> The desired product elutes after the oxidized product as indicated by the mass spectrometry data (**C, D**). The oxidized peptide ST<sub>ox</sub> (**G**) was separated from the desired peptide ST (**E**) and the expected mass was confirmed for each peptide (**F, H**) respectively. The putative oxidation of the Met residue (Met8) apparently impairs the conjugation between ST and SC (see Fig. S2B), which is in agreement with crystal structure analysis data of SC/ST001 (Fig. S3).

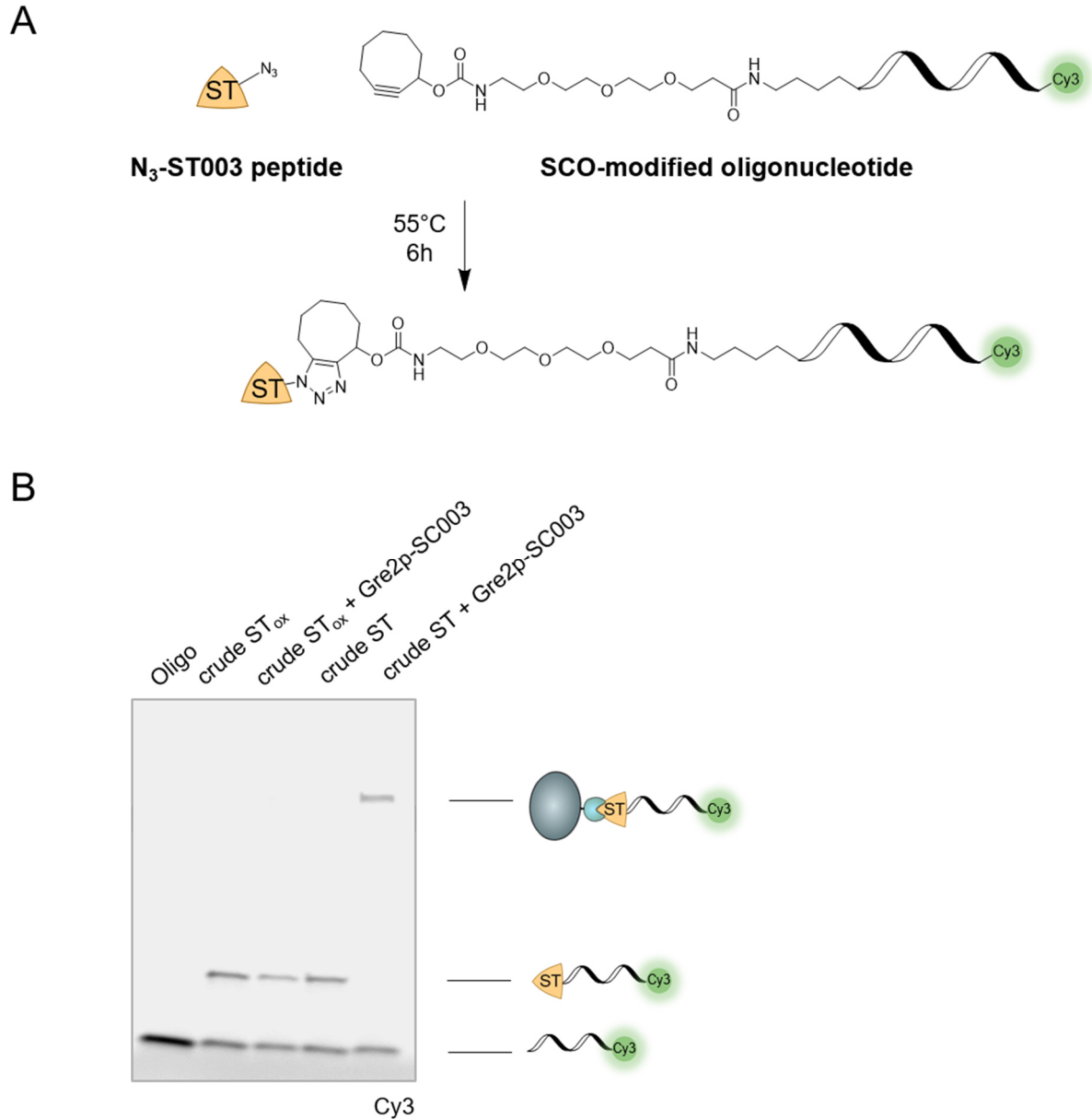


**Fig. S2 A)** Schematic illustration of the strain-promoted alkyne-azide cycloaddition (SPAAC) to synthesize the desired ST003-oligonucleotide conjugate for bioconjugation to SC-fusion proteins. **B)** Coupling of SC003 fusion protein to reaction mixtures obtained with oxidized SpyTag peptide (ST<sub>ox</sub>) and native SpyTag peptide (ST) fractions. Bands are visualized by fluorescence imaging of the incorporated Cy3-label (4-15% SDS-PAGE). The successful SPAAC reaction is confirmed by the lower electrophoretic mobility of the ST003-oligonucleotide conjugate in the reaction mixture, as compared to the unmodified staple (Oligo). Note that incubation of ST mixture with Gre2p-SC003 leads to a clear shift of the formed conjugate, whereas the ST<sub>ox</sub> mixture is not reactive with SC fusion proteins. Thus, the non-oxidized fraction was further used. Also note that the prevention of conjugation between ST<sub>ox</sub> and SC (see Fig. S2B) is presumably due to oxidation of the Met residue (Met8) (Fig. S1), which is in agreement with crystal structure analysis data of SC/ST001 indicating that Ile3 and Met5 of the ST001 peptide are located in a hydrophobic pocket formed by residues of the SC domain (Fig. S3).<sup>11</sup>



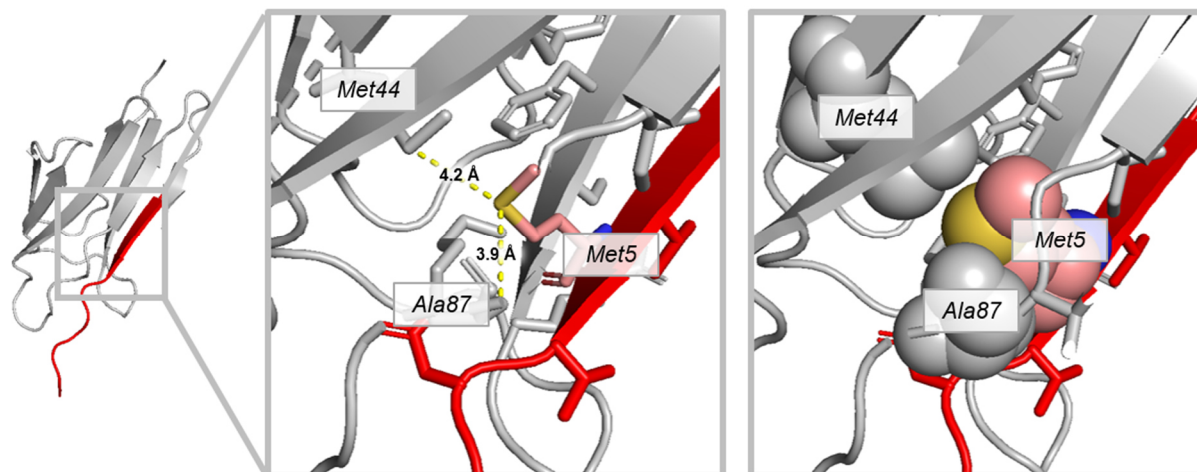


**Fig. S3** Key residues near Met5 during the SpyCatcher (grey) and SpyTag (red) interaction. This image was generated with PyMOL using the crystal structure of the SC/ST001 complex (PDB: 4MLI). The structure contains unresolved residues of SC from position 1 to 21 and 104 to 113, which are therefore also excluded from the images shown here. Note that the numbering of the amino acid residues is based on version 001, and that Met5 in the ST001 corresponds to Met8 in the ST003 peptide. Also note that the mutations introduced with the SC/ST003 variant are not located near Met5. Oxidation of Met5 in the ST peptide to methionine sulfoxide presumably leads to steric hindrance due to close proximity of the sulfur moiety (yellow) of Met5 in the ST peptide with Ala87 (3.9 Å) and Met44 (4.2 Å) inside the hydrophobic pocket created by several residues of the SC domain,<sup>4</sup> thereby disturbing the covalent coupling between ST and SC domains.

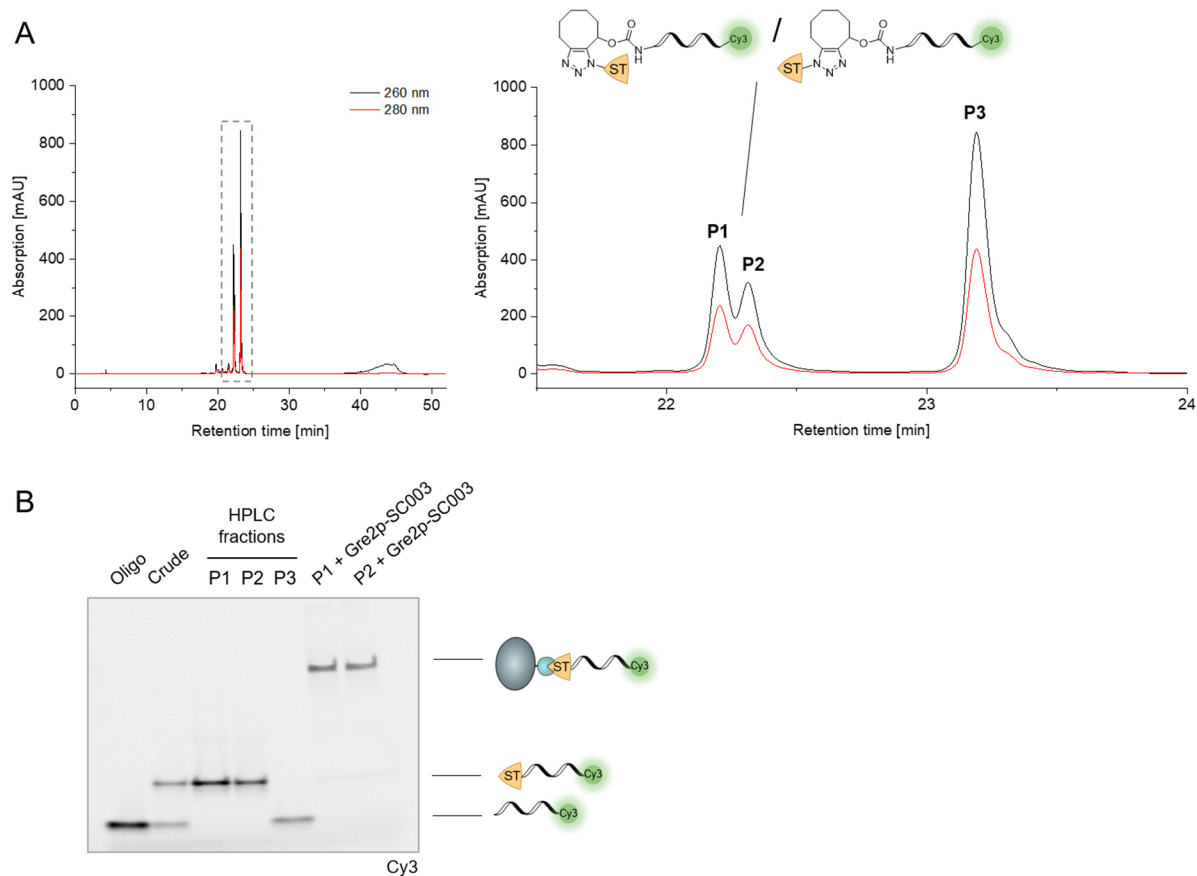


**Fig. S4** Purification of the ST-oligonucleotide conjugate. **A)** Representative HPLC chromatogram obtained from injecting the SPAAC-reaction mixture. Separation was achieved with a gradient of 5-50% acetonitrile in 0.1 M triethylammonium acetate over 30 min and products were detected at 260 nm and 280 nm. **B)** Electrophoretic analysis of pure oligonucleotide, click chemistry reaction mixture and HPLC-purified ST-oligonucleotide conjugate, as visualized by fluorescence imaging of the incorporated Cy3-label (4-15% SDS-PAGE). The successful modification and purification of the conjugate is confirmed by the lower electrophoretic mobility in fractions P1 and P2, as compared to the unmodified staple (Oligo). Fractions P1 and P2 show comparably efficient binding properties towards SC fusion proteins, as indicated by the shift upon immobilization with Gre2p-SC. The appearance of two products suggests the formation of triazole regioisomers during SPAAC synthesis (as illustrated in **A**), as previously described for these coupling reactions.<sup>12</sup> P3 represents unreacted oligonucleotide.

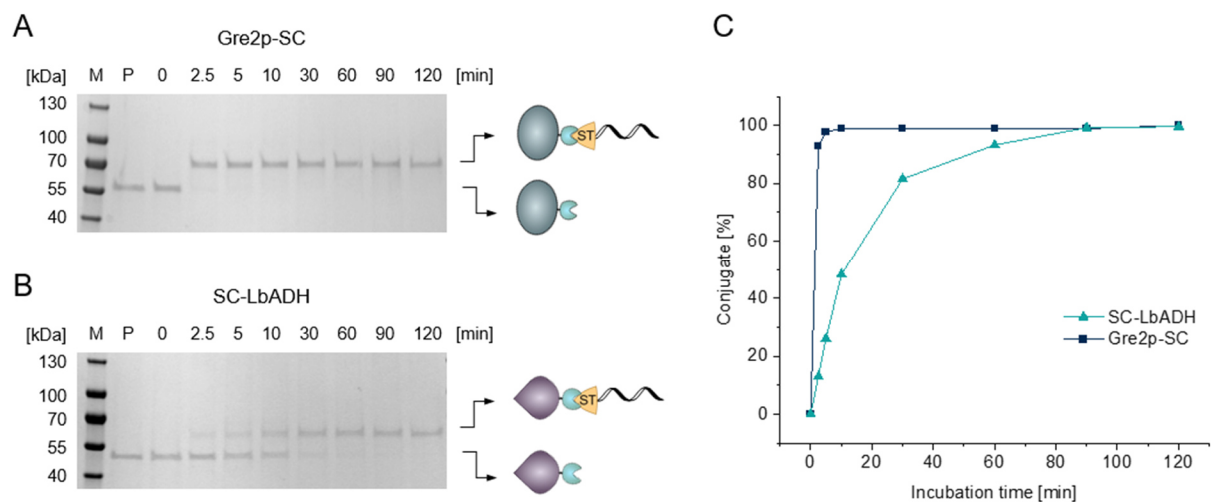


**Fig. S5** Conjugation of ST-oligonucleotide conjugate to SC-fusion proteins. **A, B**) Kinetic analysis of Gre2p-SC (51.4 kDa) and SC-LbADH (40.1 kDa) coupling to the ST-oligonucleotide conjugate. The reactions were carried out with 0.5  $\mu$ M protein and 0.65  $\mu$ M ST-oligonucleotide over the course of 120 min at 30°C (Coomassie-stained 4-15% SDS-PAGE, M = Pre-stained Protein Standard, P = protein only). **C**) Formation of protein-DNA conjugates by both SC-fusion proteins. Note that LbADH is a tetramer and equivalents were applied per monomer subunit due to accessibility of the short ST-oligonucleotide to all available SC domains. Although the coupling reaction of SC-LbADH to the ST-oligonucleotide showed a much slower rate compared to Gre2p-SC, almost complete conversion of the ST-modified oligonucleotide was achieved as well between 60 and 90 min reaction time (**B, C**). The slower coupling rate is likely due to the tetrameric structure of LbADH and the resulting steric hindrance in coupling the ST-oligonucleotide conjugate.

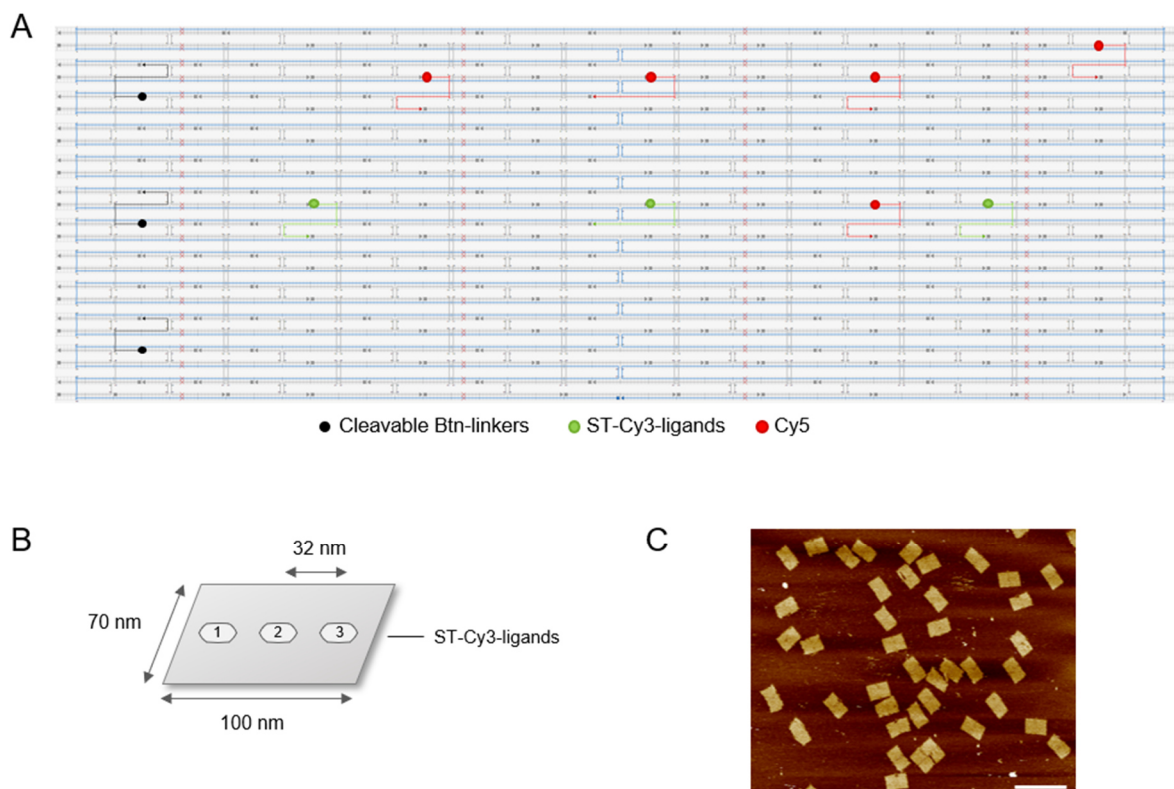


**Fig. S6** Design of DNA origami nanostructures (DON). **A)** Arrangement of DNA strands into a previously reported, rectangular DON<sup>2</sup> as illustrated using the caDNAno software.<sup>13</sup> 3'- or 5'-modified staple strands, respectively, are highlighted (black: cleavable Btn-linkers (5'-modified), green: ST-Cy3-ligands (5'-ST, 3'-Cy3), red: Cy5 (5'-modified)). The cleavable Btn-linkers were incorporated for the bead-assisted purification procedure to remove excess of protein.<sup>7</sup> **B)** Schematic illustration of the resulting DON with approximately 70 nm width and 100 nm length, exhibiting three ST-Cy3-ligands with approximately 32 nm distance for bioconjugation of SC-fusion proteins. **C)** Representative AFM image of pure DON. Scale bar: 200 nm.

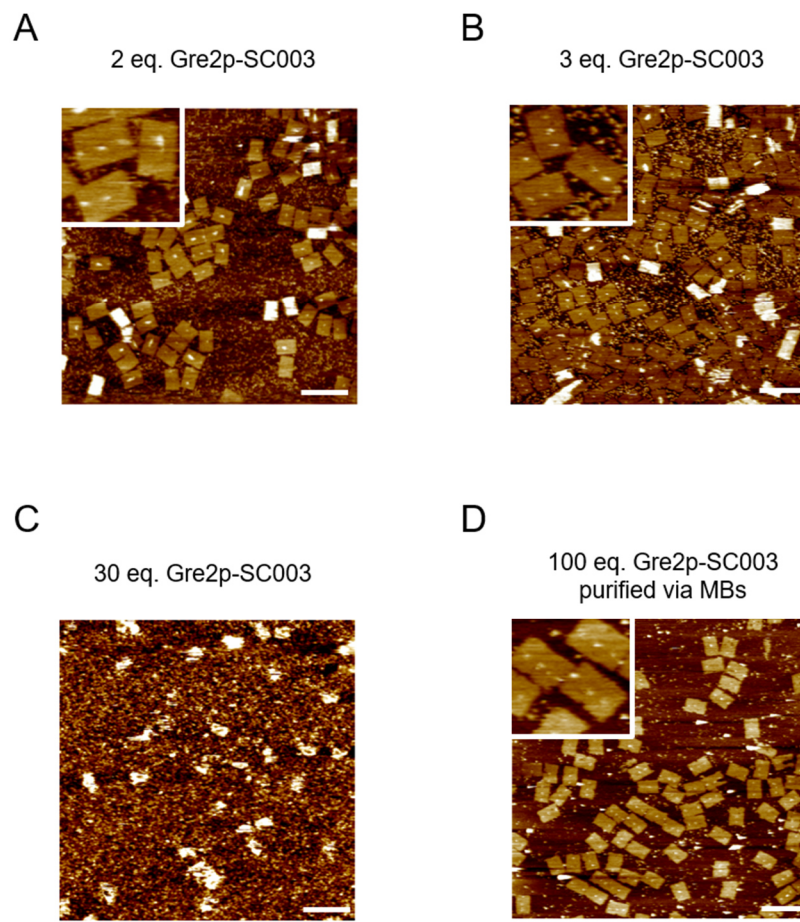


**Fig. S7** Representative AFM images of protein-decorated DON with variable equivalents of Gre2p-SC. **A)** Functionalization of DNA origami with 2 eq. Gre2p-SC, **B)** 3 eq. Gre2p-SC, **C)** 30 eq. Gre2p-SC or **D)** 100 eq. Gre2p-SC (with purification by MB), respectively, per available ST-ligand. For statistical analysis of the surface occupancies, see Fig. 2. Note that AFM imaging of crude mixtures with an excess of three **(B)** or more **(C)** molar equivalents Gre2p-SC results in a high protein background, thereby prohibiting a clear analysis of the surface occupancy on DON. Scale bars: 300 nm.

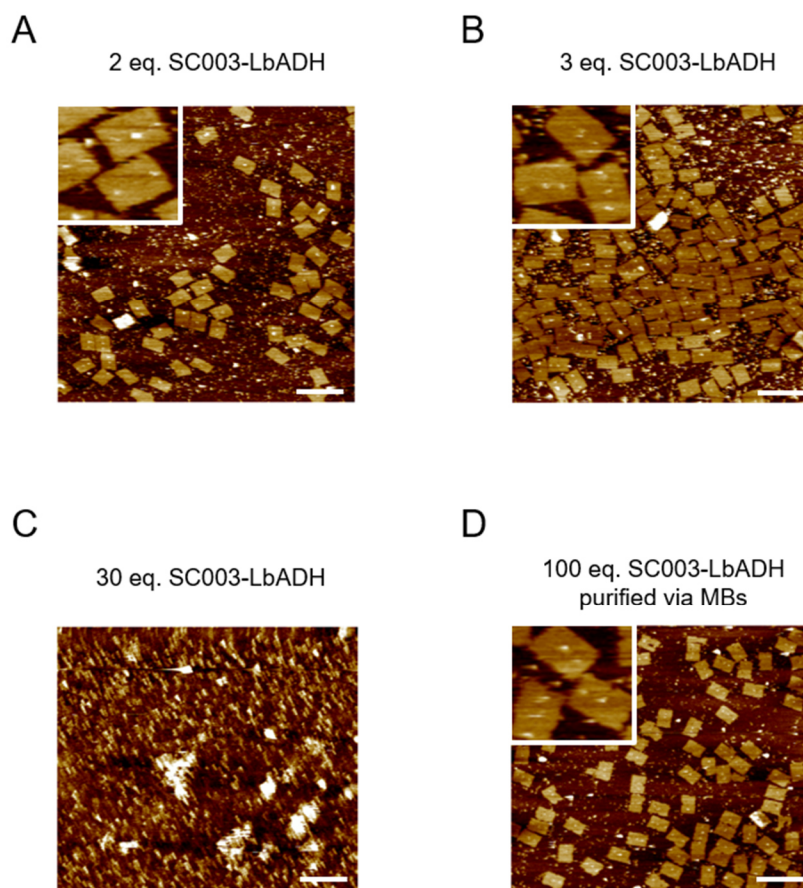


**Fig. S8** Representative AFM images of protein-decorated DON with variable equivalents of SC-LbADH. **A)** Functionalization of DNA origami with 2 eq. SC-LbADH, **B)** 3 eq. SC-LbADH, **C)** 30 eq. SC-LbADH or **D)** 100 eq. SC-LbADH (with purification by MB), respectively, per available ST-ligand. Note that LbADH is a tetramer. Since only one SpyCatcher can be accessed due to steric hindrance by the large DNA nanostructure, given equivalents are calculated per the functional form of the enzyme. For statistical analysis of the surface occupancies, see Fig. 2. Note that AFM imaging of crude mixtures with an excess of three (**B**) or more (**C**) molar equivalents SC-LbADH results in a high protein background, thereby prohibiting a clear analysis of the surface occupancy on DON. Scale bars: 300 nm.

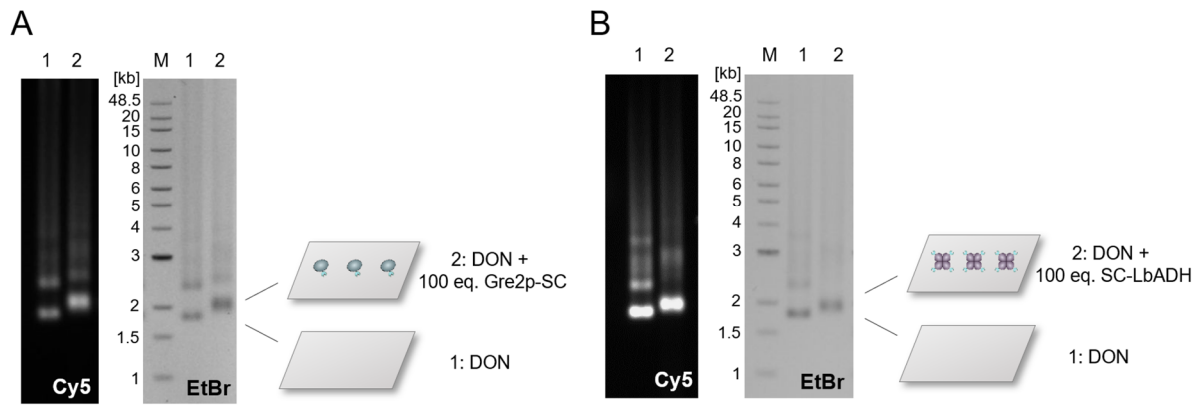


**Fig. S9** Electrophoretic analysis of protein immobilization onto ST-modified DON. **A)** 100 eq. of Gre2p-SC (lane 2) or **B)** SC-LbADH (lane 2), respectively, were allowed to bind to DON and the electrophoretic mobility was compared to pure DON (respective lane 1) on 1% agarose gels with mass reference standard (1 kb extended bp ladder). The samples were analyzed by fluorescence imaging of the incorporated Cy5-staple strands and ethidium bromide staining. Note that incubation with either Gre2p-SC (lane 2, **A**) or SC-LbADH (lane 2, **B**) results in a clear shift of the band, indicating efficient coupling of both fusion proteins.

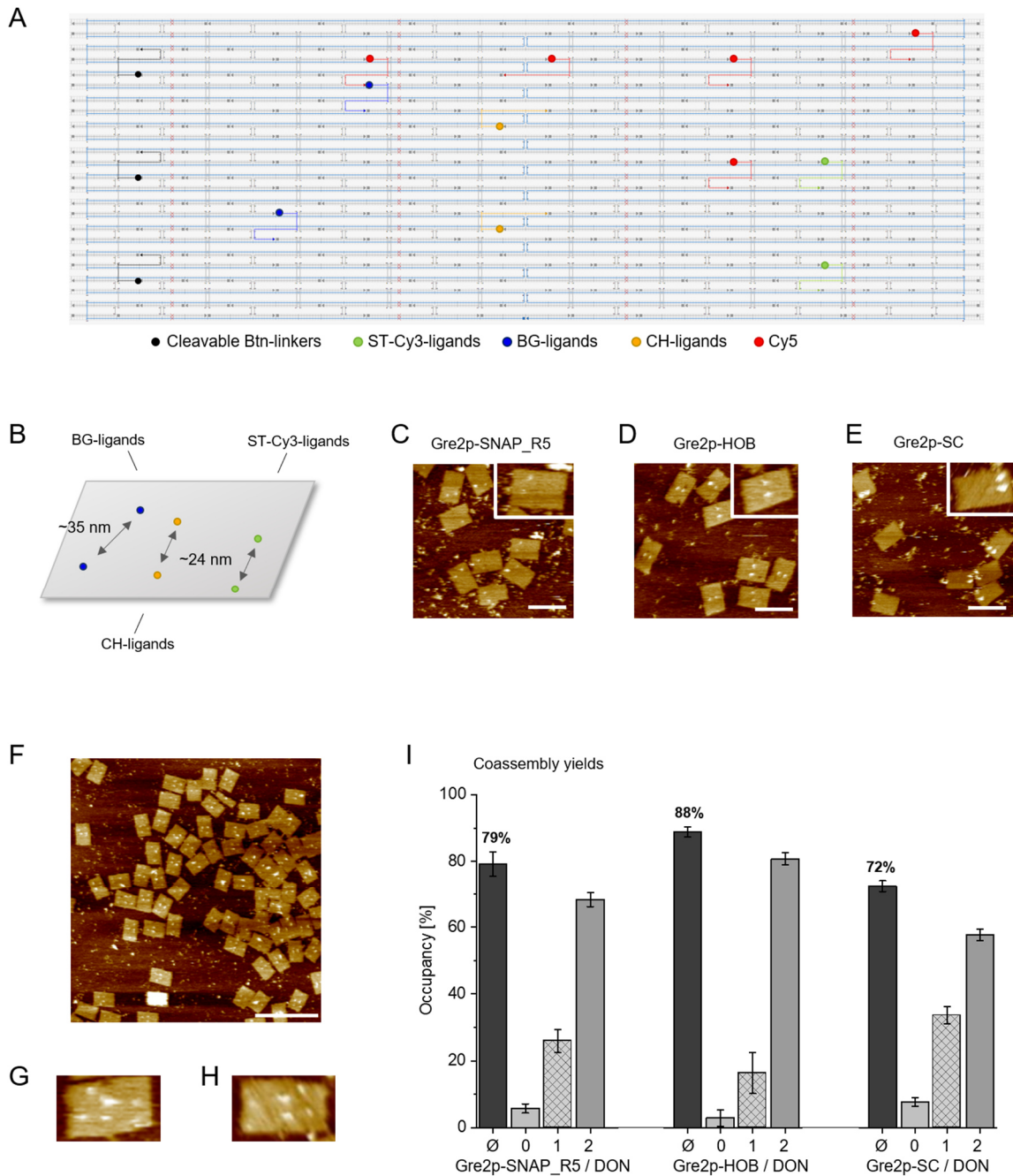


**Fig. S10** Design of DNA origami nanostructures (DON) to analyze the orthogonality of the SC-ST system to the HOB and SNAP\_R5 tags. **A**) Arrangement of DNA strands into a rectangular DON as illustrated using the caDNANO software.<sup>13</sup> Modified staple strands are highlighted (black: cleavable Btn-linkers (5'-modified), green: ST-Cy3-ligands (5'-ST, 3'-Cy3), blue: Benzylguanine (BG)-ligands (5'-modified), yellow: Chlorohexyl (CH)-ligands (5'-modified), red: Cy5 (5'-modified)). The cleavable Btn-linkers were incorporated for the bead-assisted purification procedure to remove excess of protein.<sup>7</sup> Note that the BG-, CH- and ST-ligands are arranged asymmetrically to allow clear visual discrimination of binding sites in AFM analysis. **B**) Schematic illustration of the resulting DON, bearing two BG-ligands for ligation of Gre2p-SNAP\_R5, two CH-ligands for ligation of Gre2p-HOB and two ST-Cy3-ligands for ligation of Gre2p-SC. **C, D, E**) Representative AFM images of DON incubated with either Gre2p-SNAP\_R5 (**C**), Gre2p-HOB (**D**) or Gre2p-SC (**E**). Note that neither one of the tags showed cross-reactivity with the other tags. Scale bars: 100 nm. **F**) Representative AFM image of DON decorated with a mixture containing 33 eq. of each Gre2p-SNAP\_R5, Gre2p-HOB and Gre2p-SC. Scale bar: 300 nm. Note that in



this experiment all six ligands are occupied by proteins and the resulting DON structures on the mica can be either up (**G**) or down (**H**). **I**) Average occupancy ( $\emptyset$ ) and distribution of DON with  $n = 0, 1$  or  $2$  proteins, as assessed by AFM analysis after 120 min incubation at 30°C for a total number of 160 counted DON constructs.

#### Discussion:

All three covalent connectors show efficient occupancy densities of  $\geq 72\%$ , which is consistent with previous studies of the SNAP\_R5<sup>14</sup>- and HOB-tags<sup>6</sup>. The slightly lower occupancy with the SC/ST system is most likely due to the fact that one of the ST ligands is closer to the edge of the DON compared to the other ligands used. It has previously been observed that staples located at the edges of DON show lower incorporation efficiency compared to staples located in the center of the DON.<sup>15</sup> Therefore, slightly fewer ST ligands may have been accessible in the structure than the more centrally incorporated CH and BG ligands or the ST ligands in the design from Fig. 1 in the main text.

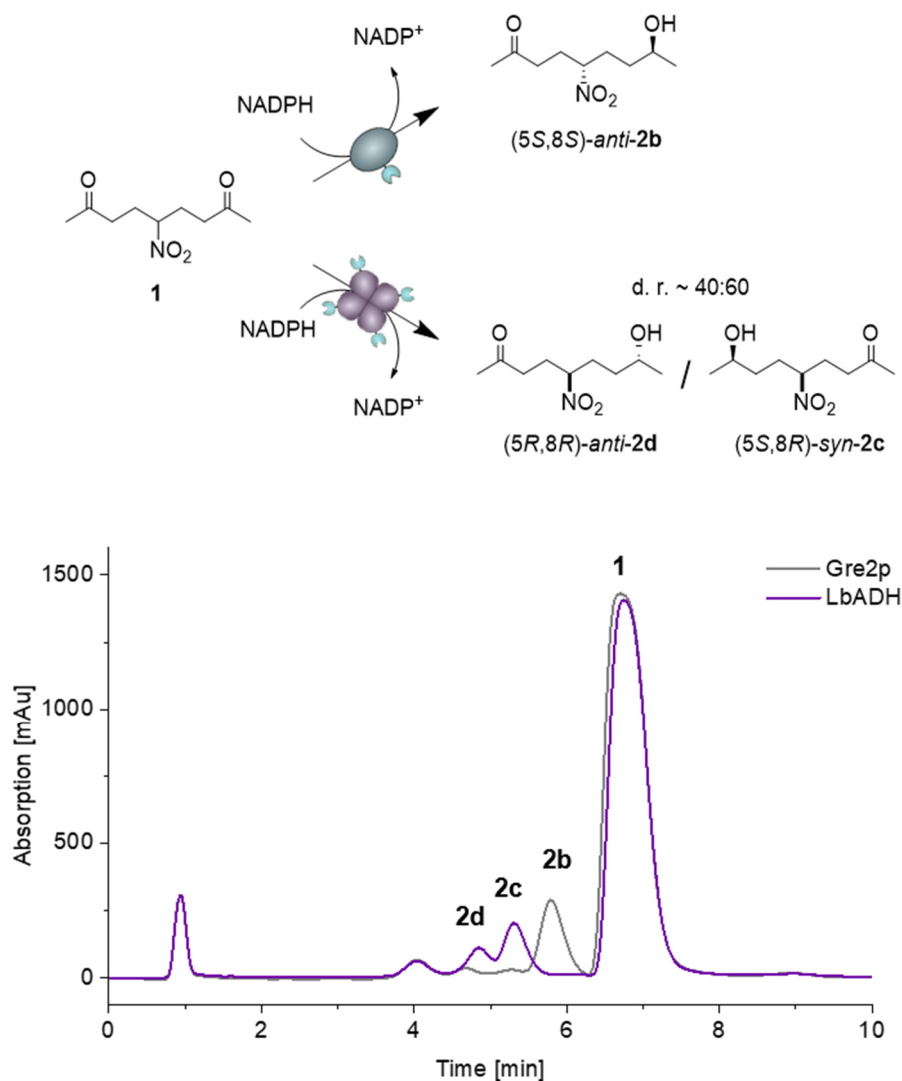


**Fig. S11** Representative HPLC chromatogram of the hydroxyketone products obtained from biocatalytic reduction of NDK **1** with Gre2p and LbADH. Gre2p performs the (*S*)-selective reduction of **1**, resulting mainly in hydroxyketone product **2b**, whereas LbADH catalyzes the (*R*)-stereoselective reduction, yielding hydroxyketone products **2c** and **2d**. The second reduction of the remaining carbonyl group leads to the corresponding (*S,S*)- or (*R,R*)-configured diols, which are however not detectable over the used reaction time. Products were analyzed using a chiral column with a 9:1 n-heptane/2-propanol mobile phase at a flowrate of 0.5 mL/min and at 10°C. All products were detected at 210 nm.

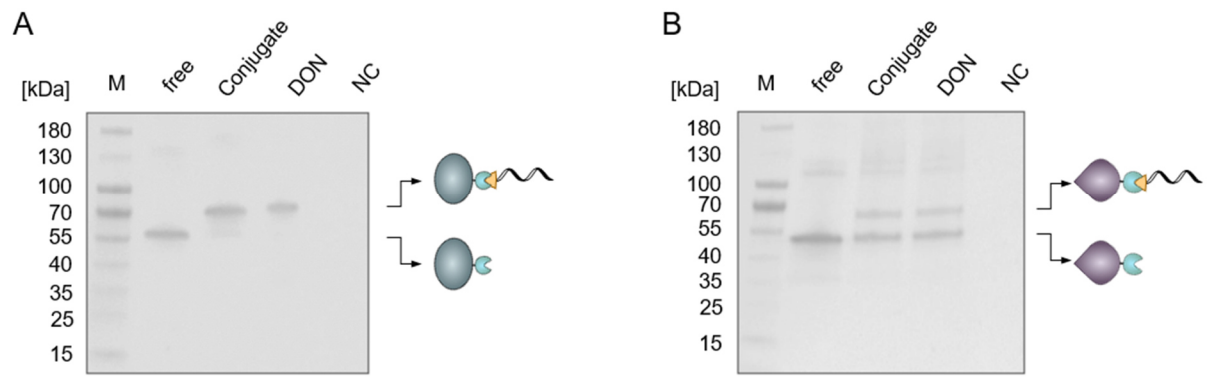


**Fig. S12** Western blot analysis of Gre2p-SC and SC-LbADH in the samples used for activity measurements. Detection of **A)** Gre2p-SC or **B)** SC-LbADH with primary rabbit-anti-SpyCatcher-antibody and secondary goat-anti-rabbit-AP antibody. The PVDF membranes were obtained by blotting of a 4-15 % SDS-PAGE with protein reference (M: Prestained protein ladder). The shift in the samples “Conjugate” and “DON” corresponds to the enzyme being conjugated to the ST-oligonucleotide or ST-modified DON, respectively. Note that LbADH forms a tetramer, resulting in a ~1:3 ratio of bound and unbound enzyme in the samples “Conjugate” and “DON”. Note that enzyme concentrations were determined before the activity experiment, and Western Blot analysis shown here serves as an additional qualitative control to ensure comparable enzyme amounts.

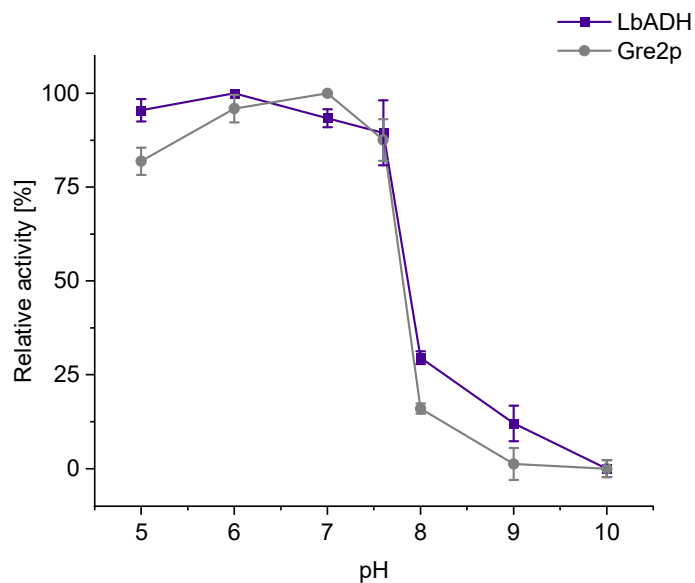


**Fig. S13** Plot of pH dependence of enzymatic activity of Gre2p-SC and SC-LbADH. Enzymatic reactions were carried out using 50 nM SC-LbADH or Gre2p-SC, respectively, with 5 mM NDK and 1 mM NADPH in buffers at different pH (5.0-10.0) containing 1 mM EDTA, 12.5 mM MgCl<sub>2</sub> and 0.01% Tween 20 at 30°C. The stability of NADPH is highly pH-dependent, with NADPH being reported to show a fast degradation between pH 3-7.4.<sup>16</sup> For this reason, and in line with previous reports on measuring the pH dependency in the context of enzyme-DON constructs,<sup>17</sup> we measured enzymatic activity in the range of pH 5.0-10.0 and subtracted the results of the negative samples, which contained no enzyme and thus only NADPH in the respective buffer, to account for possible degeneration of NADPH. Note that the pH profiles of LbADH (theoretical pI, as calculated by the Geneious software: 4.81) and Gre2p (theoretical pI: 5.08) show similar trends, with a high activity in the range of pH 5.0-7.6 and a steep decrease in activity between pH 7.6-10.0. Due to this similar trend, it is unlikely that the differences in activity upon immobilization on DON observed in Fig. 3 result from the pH dependency of the enzymes.

## Appendix

**Table S1.** Sequences of unmodified staple strands and staple strands with either Cy5-, Btn-ThiC6-, Cy3- or ST-modification, respectively, for the assembly of the rectangular DNA origami nanostructures (DON). Modifications are marked in red. ST-, CH- and BG-modifications specific for the two different DON designs are listed in Tables S2 and S3.

Name	Sequence (5'-3')
0[111]-1[95]	ACCAGTACAAACTACAACGCCTGTCAGCGGAG
0[143]-1[127]	GAACCCATGTACCGTAACACTGAGGAATTGC
0[175]-1[159]	ACCCTCATTTTCAGGGATAGCAAGAAATCTCC
0[199]-0[176]	AGAACCGCCACCCTCAGAGCCACC
0[239]-1[223]	AGGAGGTTTAGTACCGCCACCCTTTAACG
0[271]-1[255]	GTATAGCCCGGAATAGGTGTATCACCCGTATA
0[295]-1[287]	GTGCCGTCGAGAGGGTTCCGGAACC
0[327]-1[319]	AGCGGGGTTTTGCTCATTAAGAGG
0[343]-1[343]	TTTTGGATTAGGATTCCTCAAGAGAATTTTT
0[71]-2[64]	CCCTCATAGTTAGCGTGGGATTTTGCTAAATTCGGTCG
1[128]-3[127]	GAATAATAACAGCTTGATACCGATGAAGTTTC
1[160]-3[159]	AAAAAAAATATCAGCTTGCTTTTCGTGCCACTA
1[192]-2[176]	TACAGGAGAGCGTCATACATGGCTTTTAATTG
1[208]-0[200]	TAATAAGTCAGAACCGCCACCCTC
1[224]-3[223]	GGGTCAGTAAGCGCAGTCTCTGAGTTTGCC
1[24]-0[24]	TTTTTCAGACGTTAGTTGTCGTCTTTCTTTTT
1[256]-3[255]	AACAGTTAAACAAATAAATCCTCAGAACCAGA
1[288]-3[287]	TATTATTCGGCAGGTCAGACGATTAGAGCCGC
1[304]-0[296]	TGAAAGTAGTACCAGGCGGATAA
1[320]-3[319]	Cy5-CTGAGACTAGAGCCGCCAGCAGAGCCACC
1[96]-3[95]	TGAGAATAACAACAACCATCGCCCGAGGCTTT
2[111]-0[112]	CGACAATGGAAAGGAACAACATAAGTTTCGTC
2[143]-0[144]	TTCTTAAATTTTTTACGTTGACCCAATAG
2[175]-1[191]	TATCGGTTGGCTCAAAAGGAGCCTTTGATGA
2[239]-0[240]	AGAATGGAGCCTTGAGTAACAGTGCCGTACTC
2[271]-0[272]	TATCACAATGCCCCCTGCCTATTTGATATAA
2[343]-3[343]	TTTTTGAACCACCACCAGCCGCCACCATTTTT
2[47]-0[40]	AGTTAAAGAAATGAATTTTCTGTATAACGATCTAAAGTTT
2[63]-4[64]	CTGAGGCCAGCATCGGAACGAGCCGCGACC
2[79]-0[72]	CCGATATACAACCTTCAACAGTTTAGCATTCCACAGACAG
3[128]-5[127]	Cy5-CATTAAACATACCAAGCGCGAAACTCAAGAGT
3[160]-5[159]	CGAAGGCACTAAAACACTCATCTTCATTACCC
3[192]-4[176]	Cy5-TTCGGTCACTGTAGCGGTTTTTCAGAGGCAAA
3[208]-1[207]	TTATTAGCATTACCGTTCCAGTATGTAAGG
3[224]-5[223]	ATCTTTTCCGACAGAATCAAGTTAAATTCA
3[24]-2[24]	TTTTTGGGATCGTCACGCCGCTTTTGCTTTTT
3[256]-5[255]	Cy5-GCCACCACGAAACCATCGATAGCAAAGGGCG
3[288]-5[287]	CACCCTCATTACCATTAGCAAGGCAGGTAAT
3[304]-1[303]	CACCCTCATTGACAGGAGGTTGATGAAACA

3[320]-5[319]	ACCCTCAGATTAGAGCCAGCAAAAGGTGAATT
3[96]-5[95]	GAGGACTATTGTATCATCGCCTGAACAGACCA
4[111]-2[112]	ACGGAGATAAGACTTTTTTCATGAGAGTTGCGC
4[143]-2[144]	AGCGATTGGGTAAAATACGTAAAGGTGAAT
4[175]-3[191]	AGAATACACCAACCTAAAACGAAATCGGCATT
4[239]-2[240]	ATCAGTAGATAATCAAAATCACCGTTAAAGCC
4[271]-2[272]	TCACCAATCGGAACCGCCTCCCTCGGCCTTGA
4[343]-5[343]	TTTTTGCCATTTGGGACACCGACTTGATTTTT
4[47]-2[48]	<b>Btn-ThiC6</b> -AGCCGGAACCTCAGCAGCGAAAGATTGCAGGG
4[63]-6[64]	TGCTCCACCAACTTTGAAAGAGGAACTGGC
4[79]-2[80]	GTCGAAATGGTAGCAACGGCTACAACGCATAA
5[128]-7[127]	AATCTTGAAAATTGGGCTTGAGATCAGATACA
5[160]-7[159]	AAATCAACTGCCCTGACGAGAAACCATAGTAA
5[192]-6[176]	GTTTATTTAAACGCAAAGACACCATTCAGTGA
5[208]-3[207]	TCAATAGATGCCTTTAGCGTCAGATAGCCCC
5[224]-7[223]	TATGGTTTATACATACATAAAGGTAATATC
5[24]-4[24]	TTTTTCGGTCAATCATCGAGGCGCAGATTTTT
5[256]-7[255]	ACATTCAACTTATTACGCAGTATGGTTAAGCC
5[288]-7[287]	ATTGACGGAATACCCAAAAGAACTAAATAGCA
5[304]-3[303]	TCATTAAATCACCAGTAGCACCAGAACCGC
5[320]-7[319]	ATCACCGTGAAGGAAACCGAGGAATTTAAGAA
5[96]-7[95]	GGCGCATATAATCATTGTGAATTATTGAGATT
6[111]-4[112]	TTCAACTTGGCTGGCTGACCTTCAAAGTACA
6[143]-4[144]	GAGTAGTCAAGAACCGGATATTTGACCCCC
6[175]-5[191]	ATAAGGCTGTAACAAAGCTGCTCACGGAATAA
6[239]-4[240]	CGTAGAAAACCGAGCCAAAGACAGCACCGTA
6[271]-4[272]	TAAGACTCCCGATTGAGGGAGGGACGGAAACG
6[343]-7[343]	TTTTTCAAAGTTACCAAGATAGCCGAATTTTT
6[47]-4[48]	GGACGTTGAAGGGAACCGAACTGATGTTACTT
6[63]-8[64]	TCATTATCAACATTATTACAGGCGTCATAA
6[79]-4[80]	GATTTTAAGACAGATGAACGGTGTAAATTGT
7[128]-9[127]	TAACGCCAGAAGTTTTGCCAGAGGTAAGAGGA
7[160]-9[159]	GAGCAACAAAACCAAATAGCGACGTTTTAA
7[192]-8[176]	CAAAGTCAGGAGAATTAAGTAACTTACCAGA
7[208]-5[207]	TTGAGCGCTGGCAACATATAAAAGTGTACAA
7[224]-9[223]	AGAGAGATATAACATAAAAACAGAGCGAAC
7[24]-6[24]	TTTTTCTACGTTAATAGGAAGAAAAATTTTT
7[256]-9[255]	CAATAATACAAAATGAAAATAGCAGCCTTAA
7[288]-9[287]	ATAGCTATATCCAAATAAGAAACGCCAGCTA
7[304]-5[303]	AAGCCCTTACGCAATAATAACGGAAATTAT
7[320]-9[319]	AAGTAAGCTACAAAATAAACAGCCACGCTAAC
7[96]-9[95]	TAGGAATATTTAGACTGGATAGCGGTGAGAAG
8[111]-6[112]	GTA AAAATGCCACATTCAACTAATGGGTTAAT
8[143]-6[144]	TGCAAAAAAAGGAATTACGAGGACCAGAAC
8[175]-7[191]	CGACGATACTATCATAACCCTCGTACCCTGAA
8[239]-6[240]	CAGAGAGAAACCCACAAGAATTGATTAGCAA
8[271]-6[272]	TTTAACGTAGAGCAAGAAACAATGGGCATGAT
8[343]-9[343]	TTTTTAATTTGCCAGTTCCAGAGCCTTTTT

8[47]-6[48]	CCCTCAAAAAACGAACTAACGGAAACCAGTCA
8[63]-10[64]	ATATTCACAAAAATCAGGTCTTGCTCAACA
8[79]-6[80]	TGCGGAATTAGAAAGATTCATCAGCCTTATGC
9[128]-11[127]	AGCCCGAATCCTTTTGATAAGAGGCCTGTTTA
9[160]-11[159]	TTCGAGCTCAGGTCAGGATTAGAGAGCTGAAA
9[192]-10[176]	TATTCTAAATCAGATATAGAAGGCCGGAAGCA
9[208]-7[207]	GGCGTTTTGGAAGCGCATTAGACGGAGGGTAA
9[224]-11[223]	CTCCCGACAGGAATCATTACCGCAATTCTG
9[24]-8[24]	TTTTTGTTCCAGAAAACGCTTTAAACATTTTT
9[256]-11[255]	ATCAAGATGAGAACAAGCAAGCCGTGTTCCAGC
9[288]-11[287]	CAATTTTAGAACGGGTATTAACCAACAATAG
9[304]-7[303]	TCTTACCAATATTATTTATCCCACTTACCG
9[320]-11[319]	GAGCGTCTAATAATCGGCTGTCTTATATCCCA
9[96]-11[95]	CAAAGCGGCTTAGAGCTTAATTGCACCATTAG
10[111]-8[112]	GCGGATGGATTGCATCAAAAAGATGGGTAATA
10[143]-8[144]	TAATTGCAGACTTCAAATATCGGAGGCTTT
10[175]-9[191]	AACTCCAATCAAAGCGAACCAGACTTATCCGG
10[239]-8[240]	TTCATCGTTTGCGGGAGGTTTTGAAGCCTTTA
10[271]-8[272]	CACTCATCTAGTTGCTATTTTGAATTTTTTG
10[343]-11[343]	TTTTTAGAAACCAATCTACGAGCATGTTTTTT
10[47]-8[48]	ACTAAAGTGAGAATGACCATAAATTTGAATCC
10[63]-12[64]	TGTTTTACCCAATTCTGCGAACCCCTGTAAT
10[79]-8[80]	ATGCTGTATACCCTGACTATTATATCCAATAC
11[128]-13[127]	GCTATATTGCAAAATTAAGCAATACAGTCAAA
11[160]-13[159]	AGGTGGCACAATAAATCATAACAGGCGTTCTAG
11[192]-12[176]	TAAAGTACTTTCGAGCCAGTAATATAGTAGCA
11[208]-9[207]	GGTAAAGTGCCCAATAGCAAGCAAGAACGCGA
11[224]-13[223]	TCCAGACGCAACGCCAACATGTAACGCGA
11[24]-10[24]	TTTTTAAGTTTCATTACGGTGTCTGGTTTTT
11[256]-13[255]	Cy5-TAATGCAGAGTAGGGCTTAATTGAGTTAATTT
11[288]-13[287]	ATAAGTCCAAATTCTTACCAGTATTTTGAAAT
11[304]-9[303]	GAAAAATATCCTTATCATTCCAATCCTGAA
11[320]-13[319]	TCCTAATTAAGCCTGTTTAGTAGTTAAATA
11[96]-13[95]	ATACATTTAGCTAAATCGGTTGTATAAAGATT
12[111]-10[112]	GAGCATAACGCAATGGTCAATAATCATTTTTT
12[143]-10[144]	AGAATTATTCATTTGGGGCGCGAGTACCTT
12[175]-11[191]	TTAACATCTCAATTCTACTAATAGAGAGAATA
12[239]-10[240]	ATATTTAAACGACAATAAACCAACATTTTTATT
12[271]-10[272]	CGCTCAACAACGCGCCTGTTTATCAAGTACCG
12[343]-13[343]	TTTTTTAATTACTAGACACCGGAATCATTTTT
12[47]-10[48]	Btn-ThiC6-GCCTTTATCATATAACAGTTGATTAATATGCA
12[63]-14[64]	ACTTTTGTTTTAAATGCAATGCCCCCGGTT
12[79]-10[80]	ATTATGACGAGTAGATTTAGTTTGTGAATATA
13[128]-15[127]	TCACCATCAGTCTGGAGCAAACAAAACGCCAT
13[160]-15[159]	CTGATAAAAATCTACAAAGGCTATCTCCTGTAG
13[192]-14[176]	TGCAAATCTATATAACTATATGTATAGCTATT
13[208]-11[207]	AGACAAAGATTTAGGCAGAGGCATCGACAAAA
13[224]-15[223]	GAAAACCTCTACCTTTTTAACCTACAAAA

13[24]-12[24]	TTTTTGATAAAAATTTTTCAACGCAAGTTTTT
13[256]-15[255]	CATCTTCTAGTGAATTTATCAAAAATTAACAAT
13[288]-15[287]	ACCGACCGTAGCTTAGATTAAGACGGAACAG
13[304]-11[303]	AATAAGGCTCATATGCGTTATACTGAACAA
13[320]-15[319]	AGAATAAAATTTCCCTTAGAATCCGAATAACC
13[96]-15[95]	CAAAAGGGTAATCGTAAACTAGCTTGTTAAA
14[111]-12[112]	ATGAACGGTGAGAAAGGCCGGAGAAAGCCTCA
14[143]-12[144]	GCCTGAGAATATGATATTCACCAAGGCAA
14[175]-13[191]	TTTGAGAGTTAATGCCGGAGAGGGAATGCTGA
14[239]-12[240]	CTGAGAGATTTCAAATATATTTTAGAATCGCC
14[271]-12[272]	GAGTCAATGACCTAAATTTAATGGAAAGCCAA
14[343]-15[343]	TTTTTCTATTAATTAAGTAAATCGTCGTTTTT
14[47]-12[48]	CCCCAAAATTAGAACCCTCATATACGGGAGAA
14[63]-16[64]	GATAATCTTAATTTTTGTAAATGAGGGGA
14[79]-12[80]	CATATGTACTGAGTAATGTGTAGCCAAAAAC
15[128]-17[127]	CAAAAATATGACCGTAATGGGATAGGTGCGGG
15[160]-17[159]	CCAGCTTTGTCGGATTCTCCGTGGGCGAAAGG
15[192]-16[176]	ACCTGAGCAGAGGCGAATTATTCAGAGCGAGT
15[208]-13[207]	ATGATGAACCGGCTTAGGTTGGGTCAATCGCA
15[224]-17[223]	TCAAGAAATTGCTTTGAATACCAGAATTAT
15[24]-14[24]	TTTTTTATAAGCAAATCAGGAAGATTGTTTTT
15[256]-17[255]	TTCATTTGACATCGGGAGAAACAAATGGCAAT
15[288]-17[287]	TACATAAACGTCAGATGAATATACGGATTATA
15[304]-13[303]	ATGTGAGTTTGAAAACATAGCGATGTGATA
15[320]-17[319]	TTGCTTCTATAAAGAAATGCGTAAACCTACC
15[96]-17[95]	TCAGCTCAATGGGCGCATCGTAACTTCAGGCT
16[111]-14[112]	TGGTGTAGTTTTTTAACCAATAGGGAGAATCG
16[143]-14[144]	GGCGGATATTCGCGTCTGGCCTAGGTCATT
16[175]-15[191]	AACAACCCCATCAACATTAATGTTTTCAATT
16[239]-14[240]	TCGCCTGAACAAAATTAATTACATTCATAGGT
16[271]-14[272]	TACCTTTTAATTACCTTTTTTAATGCTGAGAA
16[343]-17[343]	TTTTTGAAAACAGAAATTTTGCCTTTTTT
16[47]-14[48]	CCTCAGGAATTTAAATTGTAAACGAGAAAAGC
16[63]-18[64]	CGACGACTGCCGAAACCAGGCCGCACGAC
16[79]-14[80]	TGCCAGTTAATTCGCATTAATTTATGTCAAT
17[128]-19[127]	CCTCTTCGCCAGTGCCAAGCTTTCTGTAAGCA
17[160]-19[159]	GGGATGTGTTTTCCAGTCACGACGGGGCCTT
17[192]-18[176]	ACAAAGAATGAGTAACATTATCATTGGGTAA
17[208]-15[207]	AAGGAGCGAGTTACAAAATCGCGCAAAAGAAG
17[224]-19[223]	CATCATATCTTTGCCGAACGTTGCAGCAA
17[24]-16[24]	TTTTTCAGCCAGCTTTAGATCGCACTTTTTT
17[256]-19[255]	TCATCAATTTTACAAACAATTCGAGCTGAACC
17[288]-19[287]	CTTCTGAAATAATACATTTGAGGAATCTGGTC
17[304]-15[303]	AGGGTTAGGATTTTCAGGTTAATCAATAT
17[320]-19[319]	ATATCAAATAACAATAATAGATGGAATTGA
17[96]-19[95]	GCGCAACTGGATGTTCTTCTAAGCTCTATGA
18[111]-16[112]	AGCCAGGGGTTGGGAAGGGCGATCGGTCACGT
18[143]-16[144]	ACGACGGCTATTACGCCAGCTGGAACAAAC



18[175]-17[191]	CGCCAGGGCTGCAAGGCGATTAAGTTTGCGGA
18[239]-16[240]	ATTAATCTCCTGATTATCAGATGTAACGGAT
18[271]-16[272]	TATTAGACATAATCCTGATTGTTTAGTAACAG
18[343]-19[343]	TTTTCTTTAGGAGCAATCTAAAATTTTTT
18[47]-16[48]	GCTGAATTCGGCACCCTCTGGAGTATCGG
18[63]-20[64]	TTAAGTGTCTAATCTATTTACGAATTCGT
18[79]-16[80]	AATTCATGAAAGCGCCATTCGCCACGTGCATC
19[128]-21[127]	ACTCGTCGAGGGCTTAAGCTACGTTGCGTTGC
19[160]-21[159]	GAATCGGCTCTGACCTCTGGTTGGGAAACCT
19[192]-20[176]	GCAACAGTAGGCGGTCAGTATTAATAATCATT
19[208]-17[207]	GAGAGCCAATTAATTTTAAAAGTTACCACCAG
19[224]-21[223]	ATGAAAAACGAACCACCAGCAGAATGGAAA
19[24]-18[24]	TTTTTGACAATGTCCCGTCAACCTTATTTTT
19[256]-21[255]	TCAAATATAGCCCTAAAACATCGCTCTGAAAT
19[288]-21[287]	AGTTGGCAAATGGCTATTAGTCTCCAGTCAC
19[304]-17[303]	AGTTGAAATAGAGCCGTCATAGTAATGGA
19[320]-21[319]	GGAAGGTTGTAAGAATACGTGGCATCTGGCCA
19[96]-21[95]	TACCGACAATAAAGACGGAGGATCGGTGCCTA
20[111]-18[112]	TTACCTCGGTGCGGCCCTGCCATCTCAGGAGA
20[143]-18[144]	AGTAAACGTGGGCACGAATATAGTTGTAAA
20[175]-19[191]	CTCCGAACTGACGCATTTACATACACCGCCT
20[239]-18[240]	ATACCGAATCTAAAGCATCACCTTCAACTCGT
20[271]-18[272]	GAACGATCAAACCTCAATCAATTTTAGAAG
20[343]-21[343]	TTTTTGACCTGAAAGCAGAACCCTTCTTTTT
20[47]-18[48]	<b>Btn-ThiC6</b> -TGTTTCTGCCAAAATAACCCCGCTCCTTAGT
20[63]-22[64]	AATCATGACGAGCCGGAAGCATGTTGCAGC
20[79]-18[80]	CCGAGCTCGCTCGCCCTGGAGTGATGGTTGTG
21[128]-23[127]	GCTCACTGGTTTTTCTTTTACCAGAACAAAGA
21[160]-23[167]	GTCGTGCCAGAGGCGGTTTTCGTATCCAACGTCAAAGGGC
21[192]-22[176]	GCCATTGCATATCCAGAACAATATCGGCCAAC
21[208]-19[207]	AAACGCTCAGATAAAACAGAGGTGGCCACGCT
21[224]-23[223]	TACCTACAAGAAGAACTCAAACACTACTATGG
21[24]-20[24]	TTTTTTATCCGCTCAGTGTGAAATTGTTTT
21[256]-23[255]	GGATTATTCTTTGATTAGTAATAATGCTTTCC
21[288]-23[295]	ACGACCAGCATCACGCAAATTAACAACAGGAGGCCGATTA
21[304]-19[303]	AGGGACATCAGACAATATTTTTGAATCAAC
21[320]-23[327]	ACAGAGATTCAGTGAGGCCACCGAGGAACGGTACGCCAGA
21[96]-23[95]	ATGAGTGACTGATTGCCCTCACCCCGAGAT
22[111]-20[112]	GGCAACAGGCTAACTCACATTAATGGTGCTTG
22[143]-20[144]	CAGGGTGCCCGCTTTCAGTCGGTGTAATG
22[175]-21[191]	GCGCGGGGAGCTGCATTAATGAATTACGCCCA
22[239]-20[240]	GCCTGAGTTTTTGACGCTCAATCGCATTAATA
22[271]-20[272]	CAATACTTTACATTGGCAGATTCATAATGCGC
22[343]-23[343]	TTTTTGTTTTTATAAATCCTGAGAAGTTTTT
22[47]-20[48]	GTTTGCCCAATTCACACAACATGTCATAGC
22[63]-23[71]	AAGCGGTCGGCAAAATCCCTTA
22[79]-20[80]	CTGAGAGAAAAGTGAAAGCCTGGCCCGGGTA
23[128]-22[144]	GTCCACTATTAAGAACGTGGACTTGGGCGC

23[168]-23[199]	GAAAAACCGTCTATCACGCCGCGCTTAATGCG
23[200]-21[207]	CCGCTACAGGGCGCGTATCGGCCTTGCTGGTAAACAGGAA
23[224]-22[240]	TTGCTTTGACGAGCACGTATAACGCATCACTT
23[24]-22[24]	TTTTTAATCCTGTTTGCAGCAGGCCGAATTTTT
23[256]-22[272]	TCGTTAGAATCAGAGCGGGAGCTACGTTGTAG
23[296]-21[303]	AAGGGATTTTAGACAGTAAAAGAGTCTGTCTAATAAA
23[40]-22[48]	ATGGTGGTCCGAAATCCACGCTG
23[72]-22[80]	TAAATCAAAGAATAGGCCTGGCC
23[96]-22[112]	AGGGTTGAGTGTGTTCCAGTTTGGTGAGACG

**Table S2.** Sequences of staple strands with Cy3-ST-modification for the assembly of the rectangular DNA origami nanostructures (DON) depicted in Fig S6. Modifications are marked in red.

Name	Sequence (5'-3')
11[192]-12[176]	ST-TAAAGTACTTTTCGAGCCAGTAATATAGTAGCA-Cy3
11[288]-13[287]	ST-ATAAGTCCAAATTCTTACCAGTATTTTGAAAT-Cy3
11[96]-13[95]	ST-ATACATTTAGCTAAATCGGTTGTATAAAGATT-Cy3

**Table S3.** Sequences of staple strands with Cy3-ST-modification, BG-modification or CH-modification, respectively, for the assembly of the rectangular DNA origami nanostructures (DON) depicted in Fig S10. Modifications are marked in red.

Name	Sequence (5'-3')
11[288]-13[287]	ST-ATAAGTCCAAATTCTTACCAGTATTTTGAAAT-Cy3
19[288]-21[287]	ST-AGTTGGCAAATGGCTATTAGTCTCCAGTCAC-Cy3
5[128]-7[127]	BG-AATCTTGAAAATTGGGCTTGAGATCAGATACA
15[96]-17[95]	BG-TCAGCTCAATGGGCGCATCGTAACTTCAGGCT
8[175]-7[191]	CH-CGACGATACTATCATAACCCTCGTACCCTGAA
16[175]-15[191]	CH-AACAACCCCATCAACATTAATGTTTTCAATT

**Table S4.** Primer sequences for construction of SC003-based plasmids.

Name	Sequence (5'-3')	
SK286for	GGGCAGAATAGGTGGTGGTCTGTTACCACACTGAGCGGTCTGA	Amplification of SC003 insert
SK287rev	GGCTTTGTTAGCAGCCGGATCTTAATGATGGTGGTGATGATGACC GGTATGTGCATCACCTTCGGTTG	
SK169for	GATCCGGCTGCTAACAAAGCCCGAAAGGAA	Linearization of pET22b vector backbone containing Gre2p
SK230rev	AGAACCACCACCTATTCTGCCCTCAAATT	
JH03rev	GTATATCTCCTTCTTAAAGTTAAACAAAATTATTC	Linearization of pET22b vector backbone containing LbADH
JH02for	GGTAAAGTTGCAATTATTACCGGTGG	

**Table S5.** Amino acid sequences of Gre2p-SC003, SC003-LbADH and ST003 peptide. The SC003-tag is marked in green, and the His-tag is underlined.

Name	Sequence (N-C)
Gre2p-SC003	MSV FVSGANGFIAQHIVDLLLKEDYK VIGSARSQEKAENL TEAFGNNPNFSMEIVDISKLDAFDHV FQKHGKEIKIVLHTASPFCDITD SERDLLIPAVNGVKILHSIKKYAADSVERVLTSSYAAVFDMAK ENDKSLTFNEESWNPATWESCQSDPVSAYCGSKKFAEKA AWEFLEENRDAVKFELTAVNPVYVFG PQMFDKDVKKHLNTSCELVNSLMHLSPEDKIPELFGGYIDVRDVAKAHLVAFQKRETIGQRLIVSEA RFTMQDVL DILNEDFPILKGNIPVGGKPGSGATHNTLGATLDNKKSKLLGFKFRNLKETIDDTASQIL KFEGRIGGGS <u>VTTLSGLSGEQGPSGDMTTEEDSATHIKFSKRDEDGRELAGATMELRDSSGKTIST</u> <u>WISDGHVKDFYLYPGKYTFVETAAPDGYEVATPIEFTVNEDGQVTVDGEATEGDAHTGHHHHHH</u>
SC003-LbADH	<u>MHHHHHHG</u> VTTLSGLSGEQGPSGDMTTEEDSATHIKFSKRDEDGRELAGATMELRDSSGKTISTW <u>ISDGHVKDFYLYPGKYTFVETAAPDGYEVATPIEFTVNEDGQVTVDGEATEGDAHT</u> GGGGSSNRLD GKVAITGGTLGIGLAIATKFVEEGAKVMITGRHSDVGEKA AKSVGTPDQIQFFQHDSDEDGWTKL FDATEKAFGPVSTLVN NAGIAVNKSVEETTTAEWRKLLAVNLDGVFFGTRLGIQRMKNKGLGASIIN MSSIEGFVGDPSLGAYNASKGAVRIMSKSAALDCALKDYDVRVNTVHPGYIKTPLVDDLPGAEEAM SQRTKTPMGHIGEPNDIAYICVYLASNESKFATGSEFVVDGGYTAQ
ST003 peptide	RGVPHIVMVDAYKRYK

## Literature

1. A. Kushnarova-Vakal, A. Äärelä, T. Huovinen, P. Virta and U. Lamminmäki, *ACS Omega*, 2020, **5**, 24927-24934.
2. Y. Hu, C. M. Dominguez, S. Christ and C. M. Niemeyer, *Angew. Chem. Int. Edit.*, 2020, **59**, 19016-19020.
3. P. W. K. Rothmund, *Nature*, 2006, **440**, 297-302.
4. E. Stahl, T. G. Martin, F. Praetorius and H. Dietz, *Angew. Chem. Int. Edit.*, 2014, **53**, 12735-12740.
5. D. G. Gibson, L. Young, R. Y. Chuang, J. C. Venter, C. A. Hutchison and H. O. Smith, *Nat. Methods*, 2009, **6**, 343-U341.
6. K. J. Kossmann, C. Ziegler, A. Angelin, R. Meyer, M. Skoupi, K. S. Rabe and C. M. Niemeyer, *ChemBioChem*, 2016, **17**, 1102-1106.
7. T. Burgahn, R. Garrecht, K. S. Rabe and C. M. Niemeyer, *Chem. Eur. J.*, 2019, **25**, 3483-3488.
8. M. Skoupi, C. Vaxelaire, C. Strohmann, M. Christmann and C. M. Niemeyer, *Chem. Eur. J.*, 2015, **21**, 8701-8705.
9. A. H. Keeble, P. Turkki, S. Stokes, I. N. A. K. Anuar, R. Rahikainen, V. P. Hytonen and M. Howarth, *Proc. Natl. Acad. Sci.*, 2019, **116**, 26523-26533.
10. M. Royo, G. Barany, W. Chan and P. White, in *Fmoc Solid Phase Peptide Synthesis: A Practical Approach*, Oxford University Press, 1999, ch. 4, pp. 77-114.
11. L. Li, J. O. Fierer, T. A. Rapoport and M. Howarth, *J. Mol. Biol.*, 2014, **426**, 309-317.
12. C. Ornelas, J. Broichhagen and M. Weck, *J. Am. Chem. Soc.*, 2010, **132**, 3923-3931.
13. S. M. Douglas, A. H. Marblestone, S. Teerapittayanon, A. Vazquez, G. M. Church and W. M. Shih, *Nucleic Acids Res.*, 2009, **37**, 5001-5006.
14. S. Kröll, K. S. Rabe and C. M. Niemeyer, *Small*, 2021, **17**, 2105095.
15. M. T. Strauss, F. Schueder, D. Haas, P. C. Nickels and R. Jungmann, *Nat. Commun.*, 2018, **9**.
16. J. T. Wu, L. H. Wu and J. A. Knight, *Clin. Chem.*, 1986, **32**, 314-319.
17. P. Lin, H. Dinh, Y. Morita, Z. X. Zhang, E. Nakata, M. Kinoshita and T. Morii, *Chem. Commun.*, 2021, **57**, 3925-3928.